Nanoscale

COMMUNICATION

View Article Online
View Journal | View Issue

Cite this: *Nanoscale*, 2016, **8**, 11371

Received 21st February 2016,
Accepted 3rd May 2016

DOI: 10.1039/c6nr01460g

www.rsc.org/nanoscale

Partially oxidized iridium clusters within dendrimers: size-controlled synthesis and selective hydrogenation of 2-nitrobenzaldehyde†

Tatsuya Higaki,[a] Hirokazu Kitazawa,[a,b] Seiji Yamazoe[a,b] and Tatsuya Tsukuda*[a,b]

Iridium clusters nominally composed of 15, 30 or 60 atoms were size-selectively synthesized within OH-terminated poly(amidoamine) dendrimers of generation 6. Spectroscopic characterization revealed that the Ir clusters were partially oxidized. All the Ir clusters efficiently converted 2-nitrobenzaldehyde to anthranil and 2-aminobenzaldehyde under atmospheric hydrogen at room temperature in toluene *via* selective hydrogenation of the NO_2 group. The selectivity toward 2-aminobenzaldehyde over anthranil was improved with the reduction of the cluster size. The improved selectivity is ascribed to more efficient reduction than intramolecular heterocyclization of a hydroxylamine intermediate on smaller clusters that have a higher Ir(0)-phase population on the surface.

Iridium nanoparticles (IrNPs) have been applied to various catalytic reactions such as quinoline synthesis,[1] CO_2 fixation,[2] hydrogenation[3–6] and aerobic oxidation.[7] One of the unique features of IrNPs is the bifunctionality induced by partial oxidation. For example, it is suggested that production of dimethylformamide from CO_2, H_2 and dimethylamine on partially reduced iridium oxide (IrO_x) proceeded efficiently *via* synergistic activation of H_2 and CO_2 on the surface of Ir(0) and IrO_x, respectively.[2] We previously reported that *para*-substituted nitrobenzenes with other reducible groups such as >C═O, –CHO, –CN and –Cl were efficiently and selectively hydrogenated to the corresponding aniline derivatives by using partially oxidized IrNPs (~2 nm) stabilized with PVP.[6] The high selectivity was ascribed to the preferential adsorption of the NO_2 group on the IrO_x site followed by reduction with H atoms formed by dissociative adsorption of H_2 on the Ir(0) site.[6] It was also reported that the activity and selectivity of Ir(0) particles for hydrogenation of unsaturated aldehydes to unsaturated alcohols were dramatically improved by modification with ReO_x.[8] In this regard, the partially oxidized IrNPs can be viewed as a new class of catalysts in which metal (0) NPs are partially covered by metal oxide phase.[9] However, the correlation between the structure and catalysis of Ir clusters (diameter < 2 nm) has been observed in only a few cases,[10,11] mainly due to the difficulty in their size-controlled synthesis. An open question is how the degree of oxidation and the catalytic performance of Ir clusters are dependent on the cluster size.

Dendrimers have been used as promising nanoscale vessels to generate and stabilize size-controlled metal clusters for catalytic application.[12–21] This is because a controlled number of precursor metal ions can be coordinated per dendrimer before the reduction. Recently, the size effect at the atomic level on the catalysis of Pt clusters was demonstrated using phenylazomethine dendrimers as templates.[19,21] In the present work, we synthesized Ir clusters nominally composed of 15, 30 or 60 atoms within an OH-terminated poly(amidoamine) (PAMAM) dendrimer of generation 6 (denoted as Ir : G6 hereafter). G6 was selected as a molecular container of the Ir clusters because it has enough number (256) of amine groups for coordination with Ir precursor ions and enough diameter (6.7 nm) to encapsulate the resulting Ir clusters. Ir : G6 clusters were deposited on silica[22] and applied for catalytic hydrogenation of 2-nitrobenzaldehyde. Here, we focus only on hydrogenation of 2-nitrobenzaldehyde because it is interesting to see whether or not the high selectivity toward the NO_2 group is retained when the CHO group is geometrically located even closer to the NO_2 group. We found that silica-supported Ir : G6 catalysts showed high catalytic activity for selective hydrogenation of the NO_2 group under mild conditions (30 °C, 0.1 MPa of H_2). The selectivity toward the production of 2-aminobenzaldehyde over anthranil improved with a decrease in the size.

Briefly, Ir : G6 clusters were synthesized and characterized as follows. The Ir^{IV} ions were coordinated to the amine groups of G6 by mixing the aqueous solutions of K_2IrCl_6 and G6 with the molar ratio X (X = 15, 30 or 60). Although it was reported that the Ir^{IV} ions coordinated to the PAMAM dendrimer were not reduced by either H_2 or $NaBH_4$ under ambient conditions,[4]

[a]*Department of Chemistry, School of Science, The University of Tokyo, 7-3-1 Hongo, Bunkyo-ku, Tokyo 113-0033, Japan. E-mail: tsukuda@chem.s.u-tokyo.ac.jp*
[b]*Elements Strategy Initiative for Catalysts and Batteries (ESICB), Kyoto University, Katsura, Kyoto 615-8520, Japan*

†Electronic supplementary information (ESI) available. See DOI: 10.1039/c6nr01460g

we successfully produced Ir clusters by chemical reduction using $NaBH_4$ at 60 °C. The Ir clusters thus produced will be referred to as Ir*X*:G6. For catalytic application, the as-prepared Ir*X*:G6 clusters were loaded on silica to obtain Ir*X*:G6/SiO_2. All syntheses were conducted in air. Further details on the synthesis and characterization of the Ir clusters are provided in the ESI.†

Ir*X*:G6 and Ir*X*:G6/SiO_2 clusters were characterized by UV-Vis spectroscopy, powder X-ray diffraction (PXRD), transmission electron microscopy (TEM), X-ray absorption spectroscopy, and X-ray photoelectron spectroscopy (XPS). The absorption spectra of Ir*X*:G6 (Fig. S1†) in water exhibit exponential-like profiles with a peak at ~280 nm due to the absorption of tertiary amino groups within G6.[23] The optical absorption spectra do not exhibit peaks due to Ir^{III} (352, 415 and 561 nm) or Ir^{IV} (285, 352, 415 and 561 nm) ions,[24,25] indicating that the precursor Ir^{IV} ions were completely reduced under our synthesis conditions. Nearly the same spectral profiles imply the similarity of the electronic structures of Ir*X*:G6, regardless of the difference in *X*. The PXRD patterns of Ir*X*:G6 are shown in Fig. 1a. The diffraction patterns indicate the formation of small Ir(0) nanoparticles with a face-centered cubic (fcc) crystal structure. As expected, the average size of Ir(0) crystallites estimated from the (111) diffraction peaks using the Scherrer equation increases with *X* (Table 1). The local structure of Ir in Ir*X*:G6/SiO_2 clusters was examined by analyzing the X-ray absorption fine structure (XAFS). Fig. 1b shows the Fourier-transformed EXAFS spectra at the Ir L_3 edge. The peaks in the *r* ranges of 1.45–1.85 Å and 2.23–2.95 Å are assigned to the Ir–O and Ir–Ir shells, respectively. The results of curve-fitting analysis are summarized in Table S1.† The average coordination numbers (CNs) of the Ir–Ir bond of Ir*X*:G6/SiO_2 (*X* = 15, 30 and 60) were determined to be 3.0 ± 0.5, 4.9 ± 1.0 and 6.4 ± 1.0, respectively (Table 1). The PXRD and EXAFS results clearly indicate that the cluster size was successfully controlled. Observation of the Ir–O bonds (Fig. 1b) shows that the Ir clusters were partially oxidized. The trend in which the CN values for the Ir–Ir bonds are slightly smaller than those calculated for the cuboctahedra of comparable sizes (5.5 and 7.9 for Ir_{13} and Ir_{55}, respectively) implies that the IrO_x phases were mainly formed on the surface of the Ir(0) cores rather than being distributed homogeneously over the cluster. However, the absence of diffraction peaks for IrO_x in the PXRD profiles suggests that the IrO_x phase was formed as a thin amorphous-like layer. The formation of the thin IrO_x phase on the Ir(0) core is supported by the fact that Ir*X*:G6 did not show an absorption peak at ~580 nm observed for the colloidal $IrO_x{\cdot}nH_2O$ nanoparticles (Fig. S1†).[26] The TEM images of Ir*X*:G6 (*X* = 15, 30 and 60) in Fig. 2 show the formation of monodisperse particles ~1–2 nm in diameter. The absence of larger Ir particles was confirmed by the TEM observation although accurate evaluation of the average diameters is not trivial because of the limited resolution and insufficient number (~300) of the particles observed.

The electronic structures of Ir*X*:G6 were examined by X-ray absorption near-edge structure (XANES) and XPS. In the Ir L_3 edge XANES spectra (Fig. 3), the intensity of the white lines of Ir*X*:G6 is smaller than that of K_2IrCl_6, but larger than that of bulk Ir, indicating the coexistence of Ir(0) species and the electron-deficient Ir species. Electron-deficient Ir species are presumed to be IrO_x since the absence of unreduced Ir ions is confirmed by the UV-Vis spectra (Fig. S1†). As shown in Fig. 3, the degree of electron deficiency does not depend on *X*. This

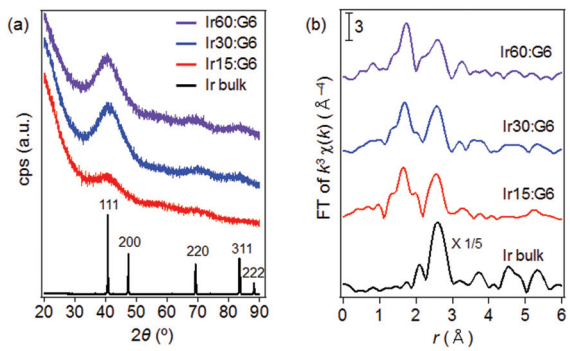

Fig. 1 (a) PXRD profiles of Ir*X*:G6 and (b) FT-EXAFS (Ir L_3 edge) of Ir*X*:G6/SiO_2 with *X* = 15, 30 and 60.

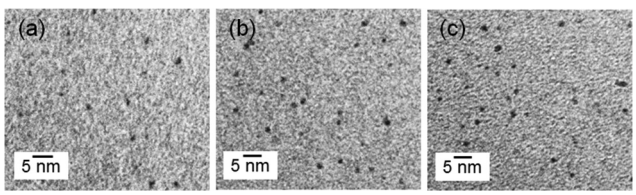

Fig. 2 Typical TEM images of Ir*X*:G6 with *X* = (a) 15, (b) 30, (c) 60.

Table 1 Structural characteristics of Ir*X*:G6

Sample	d_{XRPD}/nm	CN		BE/eV (area%)	
		Ir–Ir	Ir–O		
Ir15:G6	0.9	3.0 ± 0.5	3.5 ± 0.5	60.1 (48)	61.3 (52)
Ir30:G6	1.1	4.9 ± 1.0	4.1 ± 0.7	60.1 (43)	61.3 (57)
Ir60:G6	1.5	6.4 ± 1.0	3.6 ± 0.5	60.1 (44)	61.3 (56)

CN = coordination number, BE = binding energy of Ir $4f_{7/2}$.

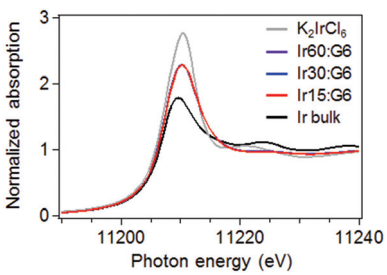

Fig. 3 XANES (Ir L_3 edge) spectra of Ir*X*:G6 (*X* = 15, 30, 60).

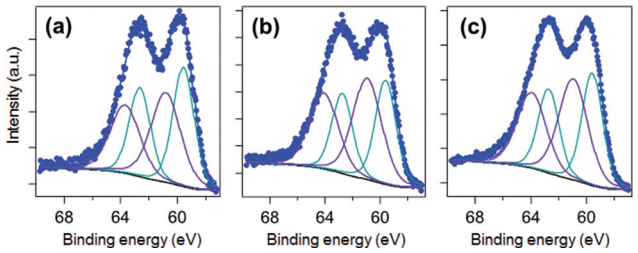

Fig. 4 XPS of IrX : G6 with X = (a) 15, (b) 30, (c) 60.

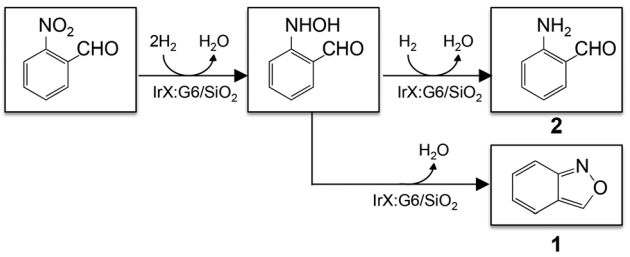

Scheme 1 Selective hydrogenation of 2-nitrobenzaldehyde catalyzed by IrX:G6/SiO_2.

trend is confirmed by the deconvolution of peaks in XPS (Fig. 4 and Table S2†): the relative population of the IrO_x phase was ~50% for all the samples (Table 1†). It is notable that the population of the IrO_x phase was independent of the cluster size although the surface-to-volume ratio decreases with the increase in cluster size. Namely, the cluster surface is not fully oxidized. If we assume that the IrO_x phase is formed only on the surface, the constant population of the IrO_x phase (Fig. 4) indicates that the population of the IrO_x phase on the surface increases with the cluster size. In summary, the IrX : G6 clusters consist of monodisperse Ir clusters and the diameter and occupancy of IrO_x on the surface increase with X.

Catalytic hydrogenation of 2-nitrobenzaldehyde was carried out using IrX : G6/SiO_2 (X = 15, 30 and 60) in toluene at 30 °C under 0.1 MPa of H_2. After 1 h, the reaction products were analyzed by gas chromatography. The results of the catalytic reaction are summarized in Table 2. Two independent batches of experiments give reproducible results and the conversion is ~100% for all the catalysts. After the reaction, 2-aminobenzaldehyde (**2**) was obtained as a major product whereas 2-nitrobenzyl alcohol (**3**) and 2-aminobenzyl alcohol (**4**) were not produced. In addition to **2**, anthranil (**1**) was formed as a by-product. It was reported that **1** is formed from 2-nitrobenzaldehyde *via* partial reduction of the NO_2 group to the NHOH group, followed by heterocyclization–dehydration reaction with the CHO group (Scheme 1).[27,28] Namely, the production of **1** is also associated with the reduction of the NO_2 group. Thus, we conclude that the NO_2 group was selectively hydrogenated even though the reducible CHO group is located at the *ortho* position of the NO_2 group. After the catalytic reaction was completed, Ir15 : G6/SiO_2 was collected by filtration. XAFS analysis for Ir15 : G6/SiO_2 thus collected shows no degradation by catalytic usage (Fig. S2†). In addition, we conducted the catalytic reaction using the filtrate under the identical conditions (ESI†). The conversion of **2** was negligibly small (<1%), indicating that the reaction did not proceed homogeneously on the leached species if any, but on the cluster surface. Namely, the results in Table 2 reflect the size-dependent catalytic properties of partially-oxidized Ir clusters.

Table 2 Catalytic hydrogenation of 2-nitrobenzaldehyde

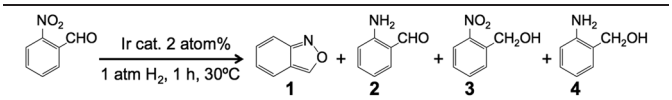

Catalyst	Conversion (%)	Selectivity (%) 1	2	3	4
Ir15 : G6/SiO_2	98	17	83	<1	0
	98	17	83	<1	0
Ir30 : G6/SiO_2	98	21	79	<1	0
	98	24	76	<1	0
Ir60 : G6/SiO_2	98	42	58	<1	0
	98	40	60	<1	0

The mechanism of selective hydrogenation of nitroaromatics to the corresponding anilines by heterogeneous metal catalysts has been extensively studied by experimental and theoretical approaches.[27–34] According to these studies, the key to the high selectivity is preferential adsorption of the NO_2 group onto highly polarized metal oxide supports *via* electrostatic interaction. It has been demonstrated that the dissociative adsorption of H_2 molecules is the rate-determining step. Based on these findings, we proposed in a previous study on Ir : PVP[6] that H atoms formed on the Ir(0) site selectively hydrogenate the NO_2 group of nitroaromatics adsorbed preferentially onto the IrO_x sites. In that study, other reducible functional groups such as –CHO and C=C located at the *para* position with respect to the NO_2 group were not reduced. Although the population of the IrO_x phase in Ir : G6 is much larger than that in Ir : PVP (~10%),[6] the selective hydrogenation observed in the present study can be explained by a similar mechanism.

Interestingly, the selectivity toward **2** over **1** increases with the decrease in cluster size. According to the proposed mechanism,[27,28] catalytic hydrogenation of the NO_2 group to the NH_2 group proceeds *via* an intermediate having a partially reduced NHOH group (Scheme 1). Product **2** is formed by subsequent hydrogenation whereas **1** is formed by intramolecular heterocyclization followed by dehydration. The rate-determining step in the overall reaction is hydrogenation of the NHOH group to form **2**.[26] Consequently, products **1** and **2** are produced competitively *via* a common hydroxylamine intermediate. Based on the XPS results (Fig. 4), the population of the Ir(0) phase on the cluster surface increased with the decrease in size. Higher selectivity for the formation of **2** by smaller clusters than larger clusters is explained by more efficient generation of H *via* dissociative adsorption of H_2 on the Ir(0)

phase. This explanation is supported by the observation that the selectivity toward **2** by Ir15G6/SiO_2 increased from 83 to 98% by increasing the H_2 pressure from 0.1 to 0.5 MPa.

Conclusions

In summary, we synthesized partially oxidized Ir clusters with nominal sizes of 15, 30 and 60 atoms by chemical reduction of Ir^{IV} ions within OH-terminated poly(amidoamine) (PAMAM) dendrimers of generation 6. The Ir clusters efficiently catalyzed the hydrogenation of 2-nitrobenzaldehyde under mild conditions (30 °C and 0.1 MPa of H_2) and yielded two products, 2-aminobenzaldehyde (**2**) and anthranil (**1**) by selective hydrogenation of the NO_2 group. The branching fraction for the formation of **2** increased with the decrease in cluster size. This size-dependent phenomenon was explained as that the reduction of the hydroxylamine intermediate proceeds more efficiently than intramolecular heterocyclization on smaller clusters having a higher population of the Ir(0) phase.

Acknowledgements

We thank Dr Shinjiro Takano and Mr Ryo Takahata for their experimental support and useful discussions. This research was financially supported by the Elements Strategy Initiative for Catalysts & Batteries (ESICB), and by a Grant-in-Aid for Scientific Research (No. 26248003) and the "Nanotechnology Platform" from the Ministry of Education, Culture, Sports, Science, and Technology (MEXT) of Japan. We thank Prof. Hiroshi Nishihara and Dr Mariko Miyachi (The University of Tokyo) for providing us with the access to the TEM apparatus. We also thank Dr Kouhei Okitsu (The University of Tokyo) for assistance with the XPS analyses.

Notes and references

1 L. He, J. Q. Wang, Y. Gong, Y. M. Liu, Y. Cao, H. Y. He and K. N. Fan, *Angew. Chem., Int. Ed.*, 2011, **50**, 10216.
2 Q. Y. Bi, J. D. Lin, Y. M. Liu, S. H. Xie, H. Y. He and Y. Cao, *Chem. Commun.*, 2014, **50**, 9138.
3 X. Zuo, H. Liu and C. Yue, *J. Mol. Catal. A: Chem.*, 1999, **147**, 63.
4 Y. M. López-De Jesús, A. Vicente, G. Lafaye, P. Marécot and C. T. Williams, *J. Phys. Chem. C*, 2008, **112**, 13837.
5 H. Rojas, G. Díaz, J. J. Martínez, C. Castañeda, A. Gómez-Cortés and J. Arenas-Alatorre, *J. Mol. Catal. A: Chem.*, 2012, **363**, 122.
6 Md. J. Sharif, P. Maity, S. Yamazoe and T. Tsukuda, *Chem. Lett.*, 2013, **42**, 1023.
7 A. Yoshida, Y. Mori, T. Ikeda, K. Azemoto and S. Naito, *Catal. Today*, 2013, **203**, 153.
8 M. Tamura, K. Tokunami, Y. Nakagawa and K. Tomishige, *Chem. Commun.*, 2013, **49**, 7034.
9 T. Mitsudome, Y. Mikami, M. Matoba, T. Mizugaki, K. Jitsukawa and K. Kaneda, *Angew. Chem., Int. Ed.*, 2012, **51**, 136.
10 I. K. Hamdemir, S. Özkar, K.-H. Yih, J. E. Mondloch and R. G. Finke, *ACS Catal.*, 2012, **2**, 632.
11 A. Okrut, R. C. Runnebaum, X. Ouyang, J. Lu, C. Aydin, S.-J. Hwang, S. Zhang, O. A. Olatunji-Ojo, K. A. Durkin, D. A. Dixon, B. C. Gates and A. Katz, *Nat. Nanotechnol.*, 2014, **9**, 459.
12 L. Balogh and D. A. Tomalia, *J. Am. Chem. Soc.*, 1998, **120**, 7355.
13 K. Esumi, A. Suzuki, A. Yamahira and K. Torigoe, *Langmuir*, 2000, **16**, 2604.
14 R. M. Crooks, M. Zhao, L. Sun, V. Chechik and L. K. Yeung, *Acc. Chem. Res.*, 2001, **34**, 181.
15 D. Astruc and F. Chardac, *Chem. Rev.*, 2001, **101**, 2991.
16 J. Zheng, P. R. Nicovich and R. M. Dickson, *Annu. Rev. Phys. Chem.*, 2007, **58**, 409.
17 C. A. Witham, W. Huang, C.-K. Tsung, J. N. Kuhn, G. A. Somorjai and F. D. Toste, *Nat. Chem.*, 2010, **2**, 36.
18 P. Maity, S. Yamazoe and T. Tsukuda, *ACS Catal.*, 2013, **3**, 182; P. Maity, S. Yamazoe and T. Tsukuda, *ACS Catal.*, 2013, **3**, 554 (corrections).
19 T. Imaoka, H. Kitazawa, W.-J. Chun, S. Omura, K. Albrecht and K. Yamamoto, *J. Am. Chem. Soc.*, 2013, **135**, 13089.
20 Z. Maeno, T. Mitsudome, T. Mizugaki, K. Jitsukawa and K. Kaneda, *Chem. Commun.*, 2014, **50**, 6526.
21 T. Imaoka, H. Kitazawa, W.-J. Chun and K. Yamamoto, *Angew. Chem., Int. Ed.*, 2015, **54**, 9810.
22 H. Lang, R. A. May, B. L. Iversen and B. D. Chandler, *J. Am. Chem. Soc.*, 2003, **125**, 14832.
23 S. Pande and R. M. Crooks, *Langmuir*, 2011, **27**, 9609.
24 A. A. El-Awady, E. J. Bounsail and C. S. Barner, *Inorg. Chem.*, 1967, **6**, 79.
25 L. Moggi, G. Varani, M. F. Manfrin and V. Balzani, *Inorg. Chim. Acta*, 1970, **4**, 335.
26 Y. Zhao, E. A. Hernandez-Page, N. M. Vargas-Barbosa, J. L. Dysart and T. E. Mallouk, *J. Phys. Chem. Lett.*, 2011, **2**, 402.
27 H.-U. Blaser, H. Steiner and M. Studer, *ChemCatChem*, 2009, **1**, 210.
28 J. Chauhan and S. Fletcher, *Tetrahedron Lett.*, 2012, **53**, 4951.
29 A. Corma and P. Serna, *Science*, 2006, **313**, 332.
30 M. Boronat, P. Concepción, A. Corma, S. González, F. Illas and P. Serna, *J. Am. Chem. Soc.*, 2007, **129**, 16230.
31 A. Corma, P. Serna, P. Concepción and J. J. Calvino, *J. Am. Chem. Soc.*, 2008, **130**, 8748.
32 K.-i. Shimizu, Y. Miyamoto, T. Kawasaki, T. Tanji, Y. Tai and A. Satsuma, *J. Phys. Chem. C*, 2009, **113**, 17803.
33 K. Shimizu, Y. Miyamoto and A. Satsuma, *J. Catal.*, 2010, **270**, 86.
34 Md. J. Sharif, S. Yamazoe and T. Tsukuda, *Top. Catal.*, 2014, **57**, 1049.

